VELOCITY MEASUREMENTS IN A THIN TURBULENT WATER LAYER

BY P. J. FINLEY *,
KHOO CHONG PHOE AND CHIN JECK POH **

Preface

This report is an account of a final year thesis project undertaken by the second and third authors with the first author as supervisor. The authors wish to thank Professor Chin Fung Kee and all those members of his staff, both academic and in the workshop, who have, in their various ways helped with this study.

1. Introduction

With the exception of boundary layer separation effects, surface tension and viscosity in the water flow on large hydraulic structures are in general negligible. Thus it is true to say that the flow, if not too complex, could be calculated on the assumption that only pressure, momentum, and gravitation effects need be considered. The majority of practical flows are very complex, so that it is common practice to construct a scale model and find an approximation to the expected flow by experiment.

A strict application of the laws of dynamic similitude would then require representative Froude, Weber, and Reynolds numbers to be the same in model and prototype. Considerations of space, time, and cost require that the model be constructed to as small a scale as possible, and that the most abundant experimental fluid, water, be used in both model and prototype. It thus becomes impossible to match the Weber and Reynolds numbers.

The surface tension of water is sufficiently low to be ignored, unless very small radii of curvature, or very low dynamic heads are involved. The incorrect representation of Weber number will not therefore be considered hereafter in this paper.

The characteristic Reynolds number in the model may however become sufficiently low for viscosity to exert a significant influence on the experimental results. The purpose of the investigation here described is to provide some basic information on a thin liquid layer dominated by viscosity. This should contribute towards providing a rational basis for the development of scaling procedures to be used in relating the results of model tests to prototypes despite the incorrect reproduction of Reynolds number.

Figure 1 shows a flat plate lying below the surface of an initially uniform stream of liquid. A boundary layer, initially laminar, grows on either side of the plate, becoming turbulent downstream. The layer on the upper surface eventually meets the free surface of the liquid. Downstream of this point the flow will be referred to as a *fully developed thin layer* and such *thin layers* form the subject of this study. The normal flat plate boundary layer on the underside of the plate will be referred to as *fully immersed.*

In the two dimensional flow of figure 1, the na-

(*) Lecturer, Department of Engineering, University of Malaya, Kuala Lumpur.
(**) Graduate, Department of Engineering, University of Malaya, Kuala Lumpur.

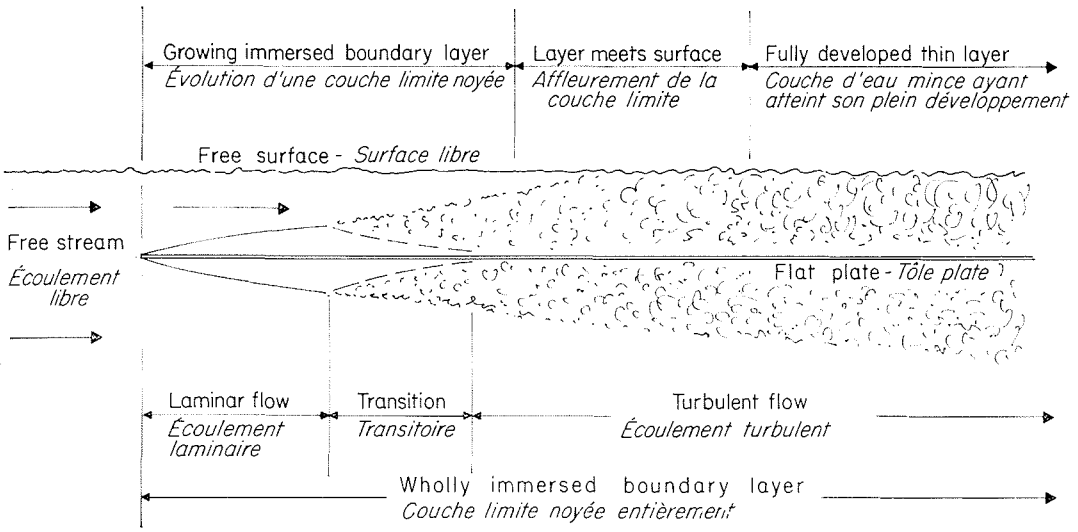

1/ Development of a thin water layer.
Evolution d'une couche d'eau mince.

ture of the flow at a given streamwise position will depend on:

x : the distance from the leading edge;
h : the depth;
u_m : the local bulk or mean velocity;
g : the acceleration due to gravity;
ρ : the liquid density;
μ : the liquid viscosity.

These variables can be formed into nondimensional groups which will be used as the determining parameters hereafter:

$\mathcal{F} = (u_m^2/gh)^{1/2}$ the Froude number;
$\mathcal{R}_h = (u_m h/\nu)$ the depth Reynolds number;
$\mathcal{R}_x = (u_m x/\nu)$ the streamwise Reynolds number.

Bauer 1953 presents measurements in thin layers of water accelerating down a spillway under the action of gravity. Measurements were not however continued downstream of the "critical point" at which the boundary layer met the free surface. Atkinson and Caruthers 1965 describe investigations of the velocity profiles in fully developed layers in both laminar and turbulent flow. Their measurements were made in relatively low velocity flows with a hot wire anemometer over a range of depth Reynolds number. The results show an experimental scatter of the order of $\pm$ 10 %.

2. Concepts from turbulent boundary layer theory

The results to be presented here will be described in relation to the generally accepted model of the flow in a turbulent boundary layer.

Near a solid surface, referred to as the *wall*, the flow depends on:

y : distance from the wall;
τ_0 : shear stress at the wall;
ρ : fluid density;
μ : fluid viscosity.

(the ratio μ/ρ is denoted by ν).

Then if a reference velocity, the *friction velocity*, u^* is defined by:

$$u^{*2} = \tau_0/\rho \tag{1}$$

dimensional analysis gives the *law of the wall*:

$$u/u^* = \underline{f}\,(yu^*/\nu) \tag{2}$$

Immediately adjacent to the wall, $yu^*/\nu < 5$, the form of $\underline{f}$ in the *laminar sublayer* is given by:

$$u/u^* = yu^*/\nu \tag{3}$$

while further from the wall in the *inner region* of turbulent flow, where $yu^*/\nu > 60$:

$$u/u^* = \mathrm{A} \log_{10} (yu^*/\nu) + \mathrm{B} \tag{4}$$

The intermediate zone, $5 < yu^*/\nu < 60$, is sometimes referred to as the *buffer zone*.

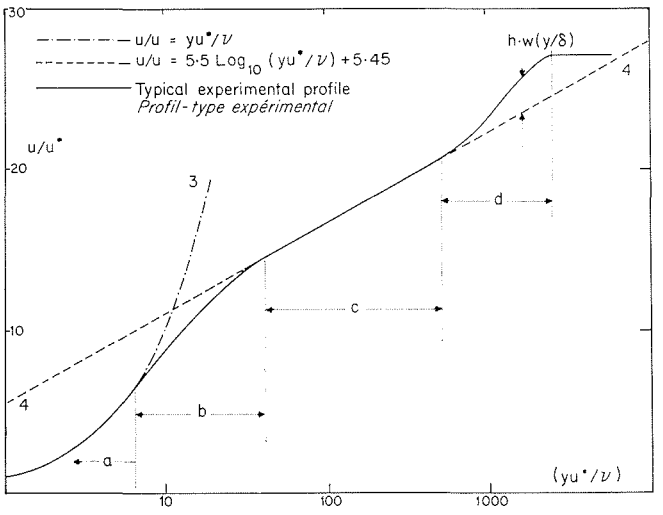

2/ Schematic velocity distribution in a wholly immersed turbulent boundary layer.
Répartition schématique des vitesses dans une couche limite turbulente noyée.

The constants A and B must be found by experiment. Sarnecki 1959 made a careful analysis of the available experimental data taking full account of Pitot displacement corrections, and found that A = B = 5.5. The values used here are those suggested by Patel 1965.

$$A = 5.5 \quad B = 5.45 \quad (5)$$

In the *outer region* of the boundary layer, approximately $y/\delta > 1/6$, where δ is the boundary layer thickness, the law of the wall is nos longer adequate. If the flow is fully turbulent and the free stream velocity is u_s then for constant pressure flows, dimensional analysis gives the *defect law:*

$$(u_s - u)/u^* = \underline{f_1}\,(y/\delta)$$

and if there is a region in which both this and 2 above apply, then the form of 4 follows. A relatively simple and general description of the flow, due in the main to Coles 1956, will be used in this paper. Coles suggested that a possible description of the whole velocity distribution was:

$$u/u^* = \underline{f}\,(yu^*/\nu) + \underline{g}\,(y/\delta, \text{...with other factors}) \quad (6)$$

and that the *divergence function* $\underline{g}$ could be expressed in the form:

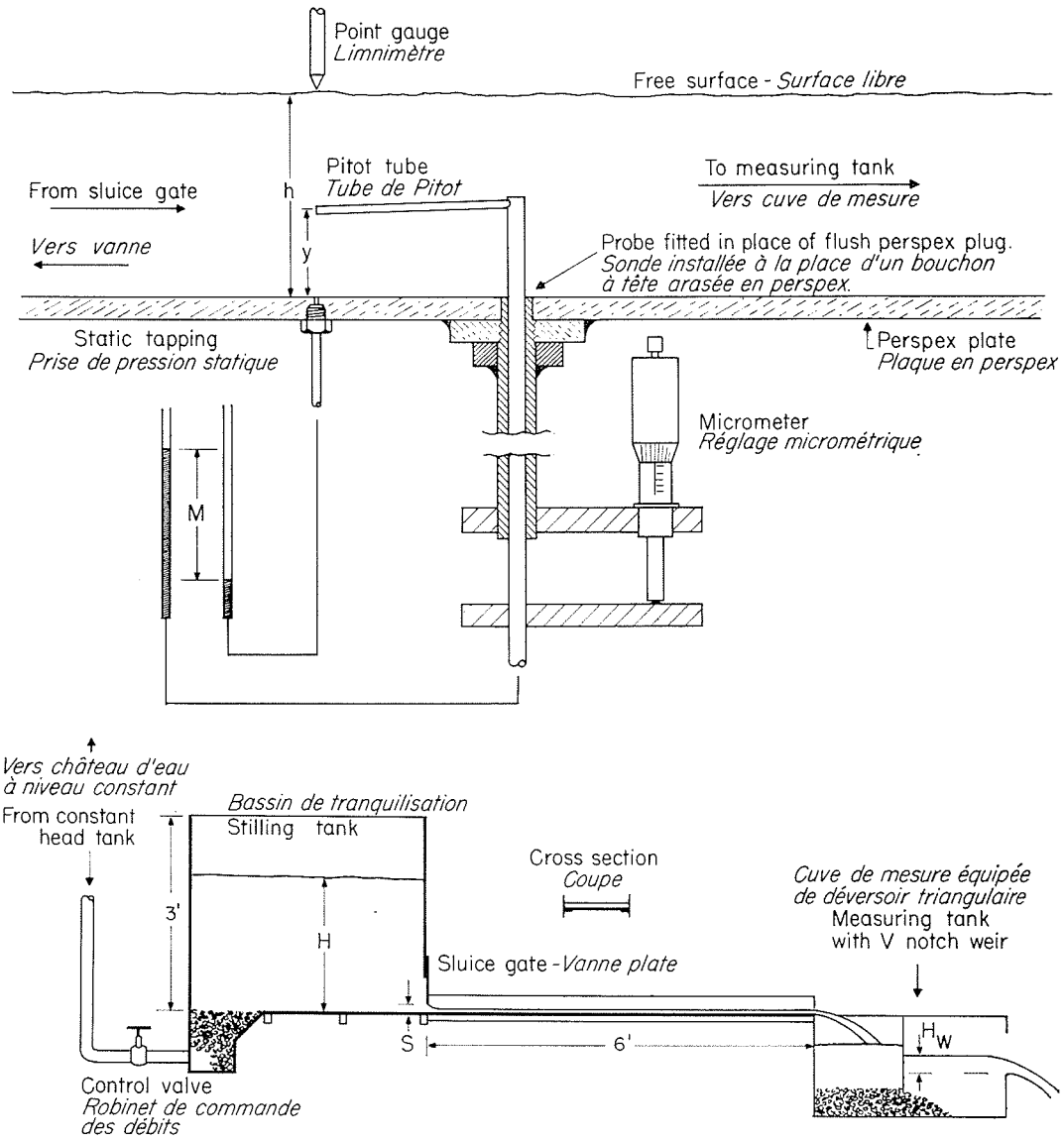

3/ Arrangement of test channel and measuring equipment.
Disposition du canal d'essai et des appareils de mesure.

$$\underline{g}\,(y/\delta, \text{other factors}) = \underline{h}\,(\text{other factors}) \times \underline{w}\,(y/\delta) \quad (7)$$

where $\underline{h}$ is a function of such variables as pressure gradient, but not of Reynolds number, and $\underline{w}$ is a universal function. This formulation has a weakness in that du/dy does not tend to zero as y tends to δ. Nevertheless Coles demonstrated that wholly submerged boundary layers can be described in this way, within the limits of experimental accuracy, for a very wide range of pressure gradients.

Figure 2 shows the complete velocity distribution as used in this paper. In the sublayer, *a*, u/u^* is given by 3, in the buffer layer, *b*, it tends from 3 to 4, and in the inner region, *c*, it is given by 4. In the outer region, *d*, the divergence function $\underline{g}$ is shown as a multiple of Coles' wake function $\underline{w}$. For a further increase in y, the velocity is constant.

Throughout this section, frequent use is made of the friction velocity u^*. It is evident that in an analysis of experimental results it will be necessary to determine u^*, or τ_0. Preston 1954 showed that the simple dimensional analysis giving 2 also implies that:

$$\tau_0 d^2/\rho\nu^2 = \underline{f_2}\,(pd^2/\rho\nu^2) \quad (8)$$

where d is the diameter of a circular Pitot tube in contact with the wall, and p is the Pitot-static pressure difference recorded. A series of very careful tests by Head and Rechenberg 1962 and Patel 1965 has established the range of reliability of the Preston tube, and the form of the function $\underline{f_2}$. Such Preston tubes, with Patel's calibration, were used in the tests here described.

3. Experimental arrangements and procedure

A thin water layer issued onto a horizontal plate from a sluice gate. The plate, of perspex, 6 feet long and one foot wide, was equipped with flush perspex plugs at 6 inch intervals along the centre-

line. At one foot intervals, a row of plugs 2 inches apart stretched across the channel. These plugs could be removed to allow a Pitot probe with traverse gear to be attached to the plate as shown in figure 3. Pairs of static holes, of 1/16 inch diameter were drilled in the plate one inch on either side of the centreline opposite the tip of the probe. The sluice gate gap varied from half an inch to one and a half inches, giving layers from one third of an inch to one inch thick. The water supply flowed from a constant head tank into a stilling tank through a stone bed. There was a lateral contraction of two to one leading to the sluice gate. As a result of this contraction and the much stronger contraction in the vertical plane as the flow approaches the sluice, it is considered that the initial boundary layer was laminar and very thin. Thus the flow downstream may be treated as initially irrotational and so equivalent to the flow on top of the plate sketched in figure 1, with the leading edge approximately at the sluice gate. The water from the plate was collected in a tank, where the temperature was measured, and after traversing another stone bed, flowed over a V-notch measuring weir into the sump.

The Pitot tubes used were one and a half inches long and 0.0312 or 0.0585 inches diameter. Their position was controlled by a micrometer screw which could be read to 0.0005 inches. A zero was established by observing the reflection of the tube in the bottom of the channel. The Pitot-static pressure difference was read on a water manometer to 0.5 mm. The depth of the layer was found with a point gauge which could be read to 0.01 inch, and a similar point gauge was used to measure the head over the V-notch weir.

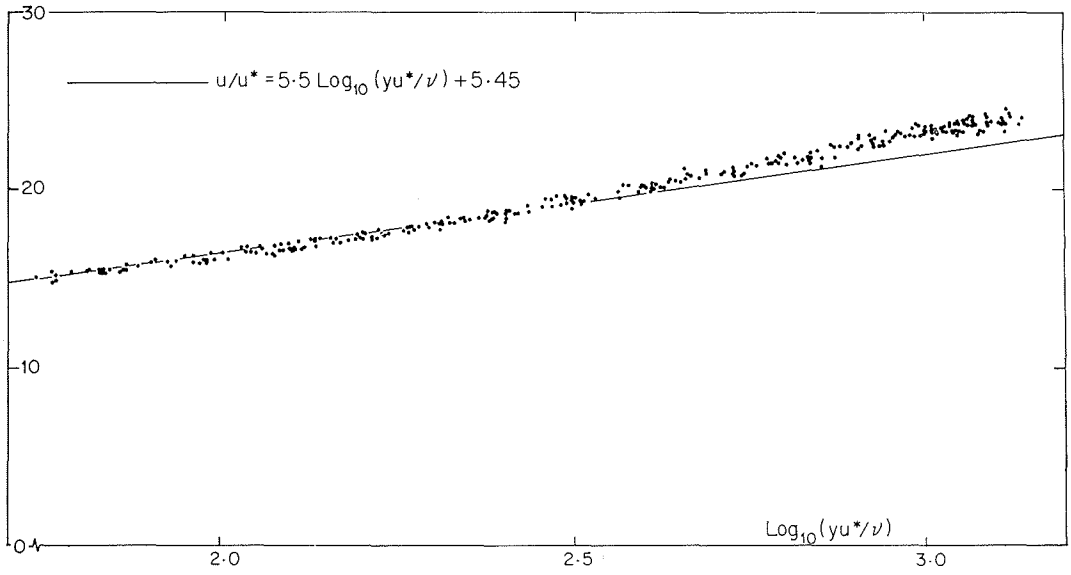

4/ Velocities observed in thin water layers plotted on an equal error basis, and compared to the law of the wall.

Vitesses observées dans les couches d'eau minces; report graphique tracé dans l'hypothèse d'erreurs égales; comparaison à la loi pour la paroi.

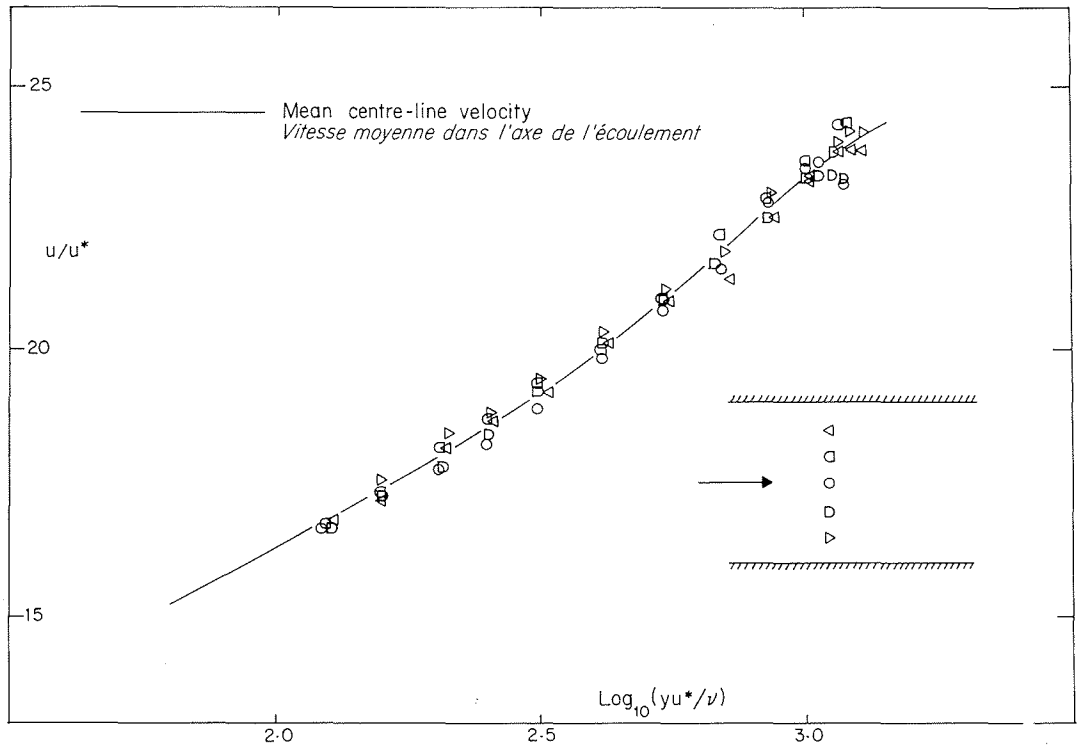

5/ Velocities observed at different stations across the channel, compared to the mean centreline distribution.

Comparaison des vitesses observées en divers points de la section de mesure avec la répartition moyenne des vitesses dans l'axe du canal.

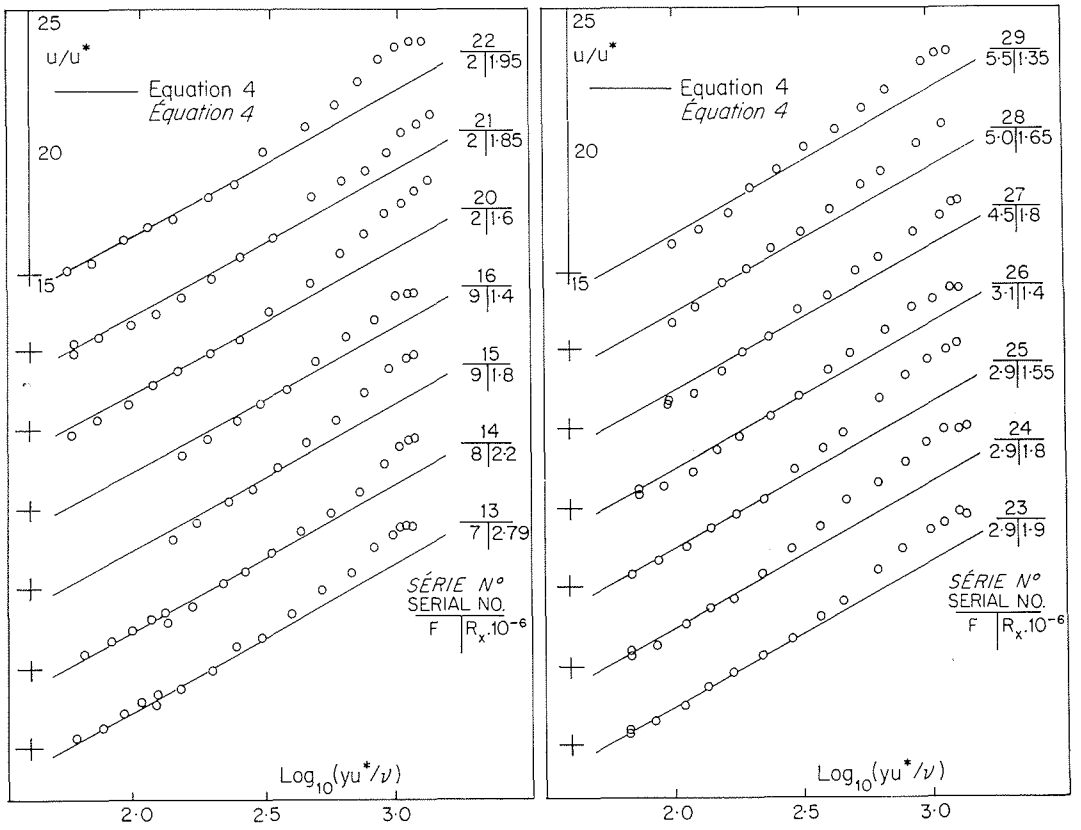

6/ Velocity profiles measured in the main tests plotted individually.

Report graphique individuel des profils des vitesses mesurées pendant les principaux essais.

Measurements consisted of a series of simple Pitot traverses. The reading with the tube in contact with the wall, which was repeated at the end of the traverse, gave a Preston tube determination of u^*. Because of irregular fluctuations of the free surface, it was found difficult to obtain readings in the uppermost part of the layer. The fluctuations cause the Pitot to break through the surface intermittently, and so give an erroneously low reading. For the same reason, the depth of the layer, h, is determined only to 0.03 inch. Readings showing a significant drop in velocity were discarded. A real drop in velocity might be caused by secondary flows, or by the retarding action of the air above the water. Since the aspect ratio of the layer was always greater than 12 : 1, the first cause was discarded. Atkinson and Caruthers calculated the likely magnitude of errors due to the second, and concluded that any drop due to this was negligible.

In this investigation a constant Pitot displacement correction of $0.17\,d$ was assumed. This, suggested by Young and Maas 1936, is an over simplification. The significance of Pitot corrections will be discussed with other factors affecting accuracy in connection with the results.

A fuller account of the equipment and procedure is given in Finley, Khoo, and Chin 1966.

4. Experimental results

Figure 4 shows a semilogarithmic plot of all the profiles recorded, compared to the inner region law of the wall in the form given by 4. The scales are chosen to give approximately equal emphasis to a given percentage error in each quantity. It can be seen that an error in y is less significant than an error in u or u^*, owing to the relatively slow increase of u/u^* with yu^*/ν. The maximum deviation from the mean u/u^* is $\pm$ 3 % while in the inner region the deviation is $\pm$ 1 1/2 %. All the measurements were made at depth Reynolds numbers $\mathcal{R}_h$ close to 3.10^4, while the Froude numbers range from 2 to 9.

Figure 5 shows a series of profiles taken across the channel using one of the transverse sets of plugs. These were obtained with natural transition and show no significant trend from the mean centreline profile. These values are also included in figure 4.

For the main series of tests a strip of sand roughness was installed, from $x = 8$ inches to $x = 10$ inches, across the full channel width. The main series of profiles is plotted individually in figure 6. The wall law is shown for comparison. Figures 4 and 6 show that there is a definite systematic tendency for the profiles to lie about 1 % below the accepted wall law in the inner region, corresponding to yu^*/ν less than about 200. This is attributed to an error in y introduced by the crude Pitot displacement correction applied. The work of MacMillan 1956 and Davies 1958 has shown that the displacement in the boundary layer is dependent on both the shear rate and the proximity of the wall. The difference in u/u^* remarked above is of the order predicted by the refined corrections of MacMillan. Since the main interest of this study however is in the outer region, the matter will not be taken further here.

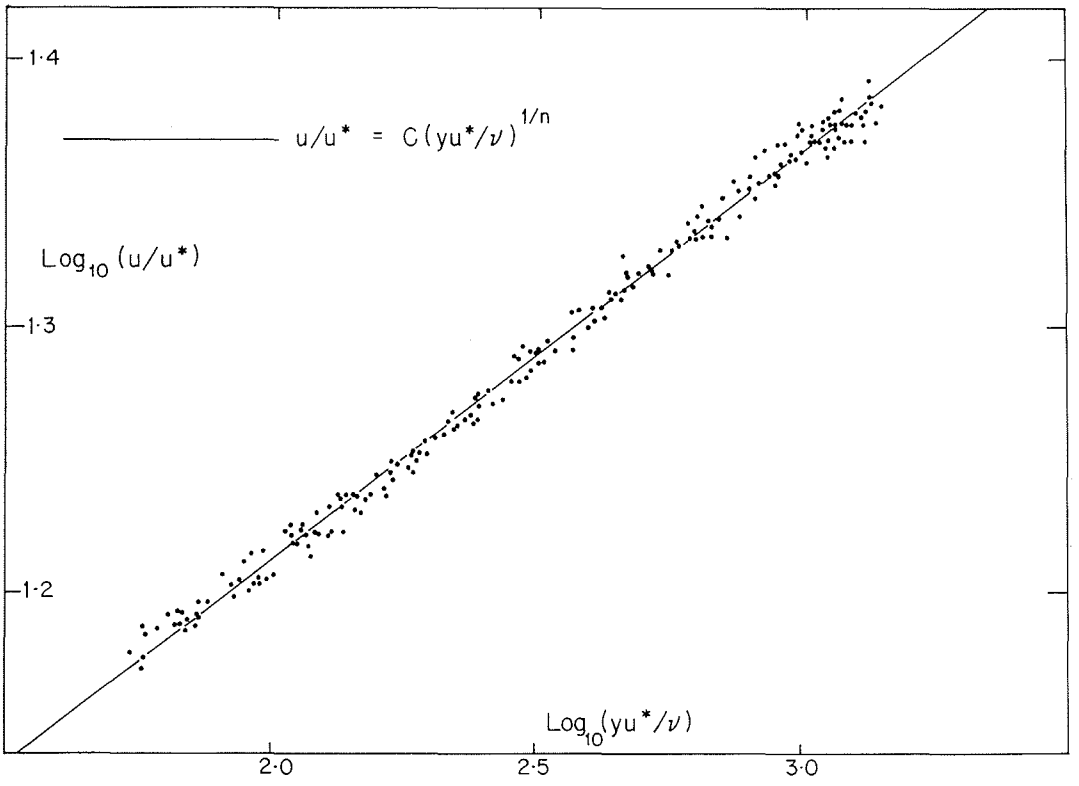

7/ Measured velocities compared with the best fitting power law
$(u/u^* = C\,(yu^*/\upsilon)^{1/n}$

Comparaison des vitesses mesurées avec la meilleure loi exponentielle de lissage
$(u/u^* = C\,(yu^*/\upsilon)^{1/n}$

The divergence from the wall law of the velocity profiles is shown clearly in figures 4 and 6. An alternative method of description commonly used is to give the velocity profile as a power law. In figure 7 the velocities of the main tests are plotted on logarithmic axes. The line represents a power law fitted by the method of least squares.
If:

$$u/u^* = C.\,(yu^*/\nu)^{1/n} \qquad (9)$$

then the line of regression is found to be given by

$$8.02 < C < 8.14 \qquad 6.5 < n < 6.61$$

Straight lines representing the limits of these figures are indistinguishable over the range plotted in figure 7, and the standard deviation of the points is 1 % in u/u^*. The deviation is greater in the outer region than in the inner region, partly due

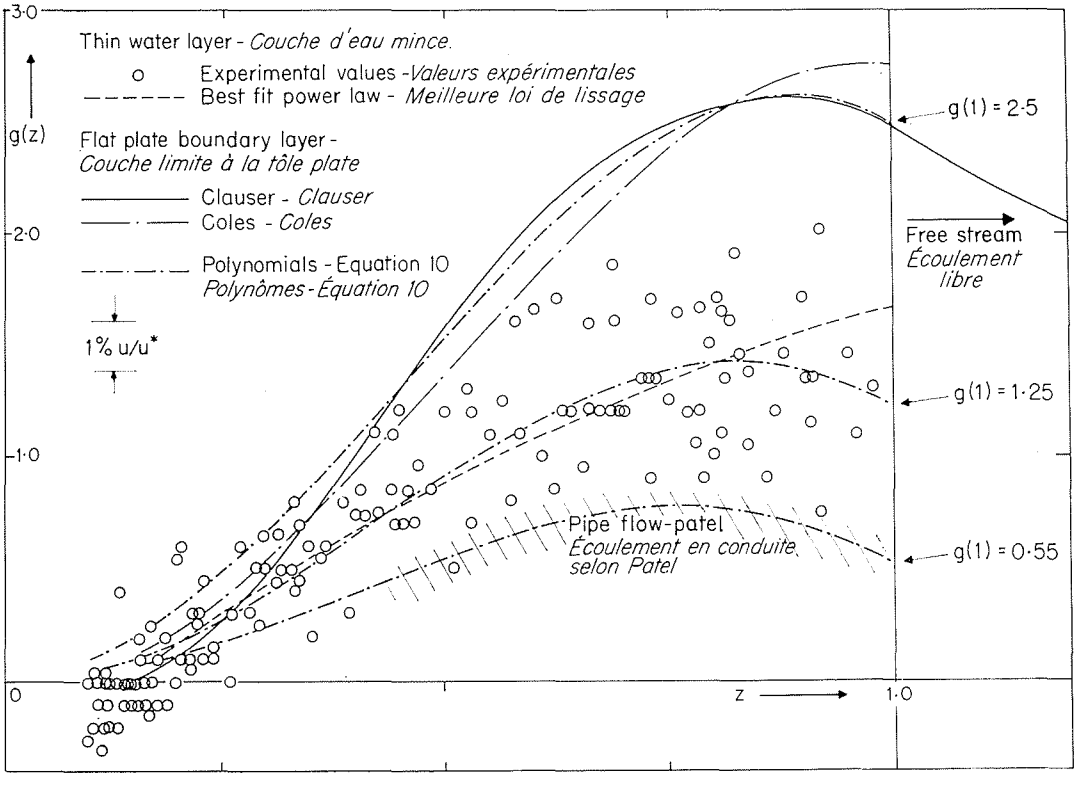

8/ Values of the divergence function g observed in thin water layers compared with previous observations in immersed boundary layers and pipe flow.

Valeurs du coefficient de divergence g observées dans des couches d'eau minces; comparaison avec des observations antérieures dans des couches limites noyées et dans l'écoulement en conduite.

to the increased scatter visible in figure 4, and partly due to the imperfections of the power law as a description of the profile. The profile as given by 9 was integrated to give the value of u_m/u^*. The friction factor c_f, where:

$$c_f = \tau_0 / (1/2\ \rho u_m^2) = 2\,(u^*/u_m)^2$$

was calculated to have the value $4.45.10^{-3}$. The value obtained from a pipe friction chart for the same Reynolds number, based on hydraulic radius and mean velocity, was $4.3.10^{-3}$.

5. Discussion

A consideration of the derivation of the wall law indicates that in this a thin water layer should show the same characteristics as a boundary layer or a pipe flow. The results quoted above support this. In the outer region however, considerable differences are observed between pipe flows and boundary layers, and the thin liquid layer may be expected to be different again. The divergence, $\underline{g}$, of the velocity profiles from the wall law, visible in figure 4, has been plotted against $y/h\ (= z)$ in figure 8. Clauser 1956 analysed the available studies of the fully immersed boundary layer, and established the form of $\underline{g}$ for the constant pressure case. This is shown in figure 8 together with the appropriate multiple of Coles' wake function $\underline{w}$. A band indicating the approximate extent of profiles in uniform pipe flow, taken from Patel's paper, is also shown.

The thin water layer profiles show a significantly different trend, $\underline{g}$ taking higher values than for pipe flow, and lower than for immersed boundary layers. Since the flow was on a horizontal plate, and retarded by friction, it is not strictly a constant pressure flow, the depth increasing and the Froude number falling downstream. The pressure gradient is very small however. Mellor and Gibson 1966 have calculated the velocity distributions of equilibrium fully immersed boundary layers as a function of the pressure gradient parameter β established by Clauser 1956. β is defined as $(\delta^*/\tau_0)\ dp/dx$ and in these tests never exceeds 5.10^{-3}. Although these are not equilibrium layers, it is suggested that Mellor and Gibson's analysis gives a good guide as to the magnitude of effects due to pressure gradient, which are indicated as a maximum change in u/u^* of 0.02. This is considered negligible within the limits of experimental accuracy. The same reservation must be made in the comparison with pipe flow, since a uniform pipe flow is of necessity in a slight favourable pressure gradient.

To provide a numerical basis of comparison the results were fitted to a polynomial satisfying the simpler boundary conditions:

$$\underline{g} = \underline{g}(z) = A'z^2\,(1 - z) + \underline{g}(1)\,z^2\,(3 - 2z) \quad (10)$$

(boundary conditions: $z = 0$, $\underline{g} = \underline{g'} = 0$; $z = 1$, $\underline{g} = g(1)$, $\underline{g'} = -A'$) in which z is the ratio y/δ, y/h, y/r, appropriate to the given type of flow, and A′ is the constant A in 4 when expressed in natural logarithms. Such polynomials satisfy the condition that du/dy should tend to zero as the edge of the layer is approached, leaving a single parameter, $\underline{g}(1)$, to specify the divergence function. It was found that:

in thin water layer flow	$\underline{g}(1) = 1.25$;
whereas in flat plate flows	$\underline{g}(1) = 2.5$;
and in pipe flows	$\underline{g}(1)$ — approx. 0.55.

The appropriate polynomials are plotted in figure 8.

The deviation of the experimental data from the best fitting polynomial is plotted in figures 9 and 10 as a function first of $\mathcal{R}_x$ and secondly of $\mathcal{F}$. The standard deviation is 1 % of u/u^*. Figure 10 shows

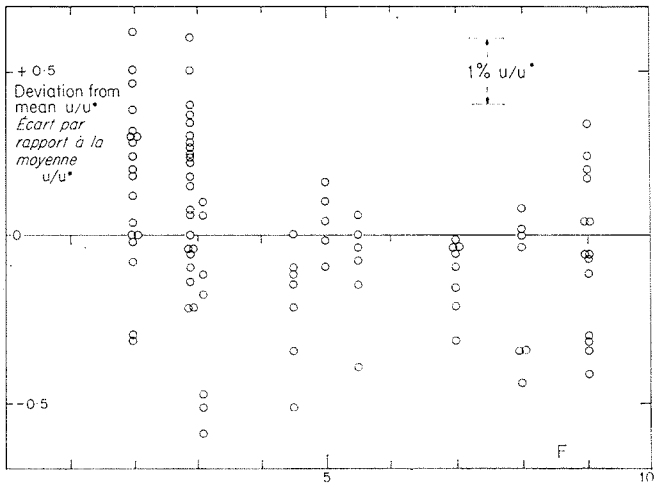

9/ Deviation of observed values of g from the best fitting polynomial 10 as function of $\boldsymbol{R_x}$.
Déviation des valeurs observées de g, *à partir du meilleur polynôme de lissage 10* f($\boldsymbol{R_x}$).

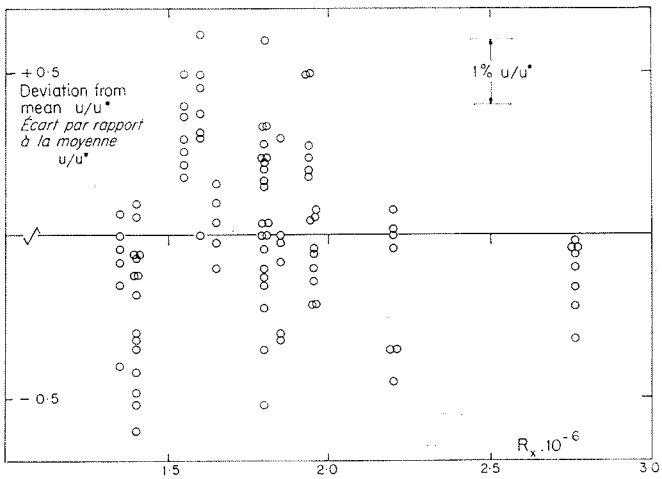

10/ Deviation of observed values of g from the best fitting polynomial 10 as function of $\boldsymbol{F}$.
Déviation des valeurs observées de g, *à partir du meilleur polynôme de lissage 10* f ($\boldsymbol{F}$).

that the profiles were obtained in a range of streamwise Reynolds number such that there is no significant dependance of $\underline{g}$ on $\mathcal{R}_x$. The experimental results thus represent a fully developed flow. Figure 10 shows that there is probably no trend with $\mathcal{F}$, in the range of experimental values, but that there may be a very slight tendency for $\underline{g}$ (1) to increase as $\mathcal{F}$ falls. Thus Froude number has a small or negligible secondary influence on the velocity distribution in the layer.

A continuing study is being undertaken in which measurements are to be made in water layers flowing up and down slopes, and over a range of depth Reynolds numbers.

6. Conclusion

The velocity profile in a fully developed horizontal water layer, when described in suitable nondimensional terms, is shown to be independent of the Froude number. In the inner region the law of the wall describes the velocity well. In the outer region, the divergence of the velocity from the wall law is about half that observed in constant pressure boundary layer flows, and twice that observed in uniform pipe flow.

List of symbols

A, B constants in the 'wall law' (Eq. 4);
C constant in the 'power law' (Eq. 9);
$\mathcal{F}$ Froude number;
$\mathcal{R}_h$ Reynolds number based on depth;
$\mathcal{R}_x$ Revnolds number based on distance from sluice gate.

Functions describing boundary layer effects:—

$\underline{f}$ wall law function (Eq. 2);
$\underline{f_1}$ defect law function;
$\underline{f_2}$ preston tube calibration function (Eq. 8);
$\underline{g}$ divergence function (Eq. 6);
$\underline{h}$ Coles' scaling function (Eq. 7);
$\underline{w}$ Coles' wake function (Eq. 7);

c_f skin friction coefficient;
d diameter of Preston tube;
g acceleration due to gravity;
h depth of layer;
n exponent in power law (Eq. 9);
p pressure difference recorded by Preston tube;
r radius of pipe;
u velocity;
u^* friction velocity (Eq. 1);
u_m mean or bulk velocity;
u_s surface or free stream velocity;
x distance from sluice gate;
y distance normal to solid boundary;
z proportion of layer thickness ($= y/\delta$, y/h, y/r);
β Clauser's outer region pressure gradient parameter;
δ boundary layer thickness;
δ^* displacement thickness of layer;
μ viscosity of fluid;
ν kinematic viscosity;
ρ density of fluid;
τ_o wall shear stress.

References

Atkinson (B.) and Caruthers (P. A.). — Velocity profile measurements in liquid films. *Trans. Instn. Chem. Engrs.*, 43 (1965), T 33.

Bauer (W.). — The development of the turbulent boundary layer on steep slopes. *Proc. Amer. Soc. Civ. Engrs.*, separate No. 281, (1953).

Clauser (F. H.). — The turbulent boundary layer. *Advances in applied mechanics*, 4, Academic Press, New York, (1956).

Coles (D.). — The law of the wake in the turbulent boundary layer. *J. Fluid Mech.*, 1 (1956), 191.

Davies (P. O. A. L.). — The behaviour of a Pitot tube in transverse shear. *J. Fluid. Mech.*, 3 (1958), 441.

Finley (P. J.), Khoo Chong Phoe and Chin Jeck Poh. — Velocity measurements in a thin turbulent water layer. *Jour. Engrg. Dept.*, 5, University of Malaya, (1966).

Head (M. R.) and Rechenberg (I.). — The Preston tube as a means of measuring skin friction. *J. Fluid Mech.*, 14 (1962), 1.

McMillan (F. A.). — Experiments on Pitot tubes in shear flow. *Aero. Res. Counc.*, R. and M., No. 3028 (1956).

Mellor (G. L.) and Gibson (D. M.). — Equilibrium turbulent boundary layers. *Journal of Fluid Mechanics*, 24 (1966), 225.

Patel (V. C.). — Calibration of the Preston tube and limitations on its use in pressure gradients. *J. Fluid Mech.*, 23 (1965), 185.

Preston (J. H.). — The determination of turbulent skin friction by means of Pitot tubes. *J. Roy. Aero. Soc.*, 58 (1954), 109.

Sarnecki (A. J.). — Ph. D. Thesis, Cambridge University, (1959).

Young (A. D.) and Maas (J. N.). — The behaviour of a Pitot tube in a transverse total pressure gradient. *Aero. Res. Counc.*, R. and M., No. 1770 (1936).

Résumé

Mesure des vitesses dans une mince couche d'eau turbulente

par P. J. Finley *, Khoo Chong Phoe * * et Chin Jeck Poh * *

Pour établir une corrélation rationnelle entre les résultats d'essais sur modèles hydrauliques, et l'écoulement susceptible de se produire dans la nature, il est nécessaire de bien comprendre les écoulements correspondant à des nombres de Reynolds relativement faibles, tels qu'ils se présentent sur les modèles réduits. La présente étude examine l'écoulement de l'eau sur une surface horizontale; on montre, dans une première partie, que les paramètres significatifs sont les nombres de Froude et de Reynolds, compte tenu de la profondeur, et de la distance de l'origine, de la tranche d'eau considérée.

On examine les lois de similitude correspondant à une couche limite à deux dimensions, et entièrement immergée, et l'on adopte la définition à deux composantes, proposée par Coles en 1956 :

$$u/u^* = \underline{f}\,(yu^*/\nu) + \underline{g}\,(y/\delta) \qquad (6)$$

Si l'on admet que les lois classiques de l'écoulement à la paroi, et de la vitesse déficitaire, pour une couche limite turbulente, sont valables pour la couche liquide de faible épaisseur, les fonctions $\underline{f}$ et $\underline{g}$ seront indépendantes du nombre de Reynolds (deuxième partie de l'étude).

On a mesuré une série de profils de vitesse à l'intérieur de tranches d'eau de faible épaisseur (0,85 cm - 2,5 cm), s'écoulant d'une vanne de pertuis sur une plaque horizontale (voir la figure 3 *b*). Les vitesses ont été déterminées par des mesures soigneusement exécutées à l'aide d'un tube de Pitot, et l'effort de cisaillement au fond a été mesuré en employant un tube de Pitot comme tube de Preston (troisième partie de l'étude). Ces mesures ont été effectuées en fonction d'un nombre de Reynolds, dans le sens de la profondeur, égal à 3.10^4, et les résultats obtenus se sont présentés sous la forme d'une courbe unique, dont l'écart-type était inférieur à 1 % (voir les figures 4 et 7).

La zone intérieure du profil est bien conforme à la loi logarithmique d'écoulement à la paroi, compte tenu des constantes proposées par Patel en 1965 (voir les figures 4 et 6). Les quelques faibles écarts résiduels proviennent sans doute de l'insuffisance des coefficients appliqués aux résultats de mesure pour tenir compte de la proximité du fond (quatrième partie de l'étude). Au-dessus de la tranche intérieure, dont l'épaisseur correspond au cinquième de celle de l'ensemble de la couche, l'écart entre les résultats et la loi de paroi augmente progressivement, et les résultats présentent une dispersion un peu plus accentuée que dans la zone intérieure. On propose une forme polynôme simple pour la fonction de divergence $\underline{g}$, qui vérifie les conditions aux limites simplifiées :

$$\underline{g}\,(z) = A'z^2\,(1 - z) + \underline{g}\,(1)\,z^2\,(3 - 2\,z) \qquad (10)$$

avec $z = y/\delta$, A' étant une constante universelle, et $\underline{g}\,(1)$ correspondant à la valeur de $\underline{g}$ au bord extérieur de la couche, servant comme paramètre unique, et caractérisant le profil. Cette fonction de divergence dans les couches-limite à charge constante, et entièrement immergées, pour lesquelles la valeur de $\underline{g}\,(1)$ est de l'ordre de 2,5, et pour le cas d'un écoulement uniforme dans une conduite, où la valeur de $\underline{g}\,(1)$ est de l'ordre de 0,55 (cinquième partie de l'étude). Les résultats ont été adaptés à 10, par la méthode des moindres carrés; on a pu constater que la meilleure adaptation correspondait au cas où $\underline{g}\,(1) = 1{,}25$ (voir la figure 8). Les résultats ont alors été portés en fonction du nombre de Reynolds dans le sens du courant, à titre de vérification (voir la figure 9), et aucune corrélation n'a pu être décelée. Par conséquent, les mesures avaient été effectuées dans des couches bien établies. Si l'on porte ces résultats en fonction du nombre de Froude (fig. 10), il apparaît que la fonction $\underline{g}$ ne dépend que peu, ou dans une mesure négligeable, du nombre de Froude, tant que les valeurs de ce dernier se situent entre 2 et 9.

* Lecturer, Department of Engineering, University of Malaya, Kuala Lumpur.
** Graduate, Department of Engineering, University of Malaya, Kuala Lumpur.